scientific reports

Check for updates

OPEN

Mechanistic investigation into the performance of stone columns constructed with riverbed aggregates in varied soil conditions

Ahmed Almutairi

Stone columns are an efficient and economical ground improvement technique to enhance weak soils' bearing capacity and settlement behaviour. This experimental study examines the performance of stone columns constructed with riverbed gravel as a sustainable alternative to conventional crushed stone in layered soil conditions. Laboratory-scale plate load tests were conducted in a cylindrical unit cell of soft clay, silt, and sand layers. Two identical stone columns (63 mm diameter, 250 mm length) were installed and tested under two loading conditions: entire cross-sectional and column-only loading. Results indicated that stone column installation significantly increased load-bearing capacity by up to 43% in clay, 25% in silt, and 27% in sand compared to untreated soils. In layered soil, the improvement reached approximately 34%. Columns constructed with riverbed gravel achieved 80–95% of the performance of those using crushed stone, demonstrating comparable stiffness and settlement reduction, though with slightly greater bulging near the surface. The study confirms that riverbed gravel offers a cost-effective and sustainable alternative for stone column applications, maintaining high structural efficiency while reducing environmental impact.

Keywords Stone column, Riverbed gravel, Load–settlement behaviour, Bulging, Layered soil, Ground improvement

Rapid advancements in civil and geotechnical engineering have accelerated infrastructure growth worldwide, leading to an increasing demand for stable construction sites[1,2]. However, the availability of suitable land with favorable geotechnical conditions is rapidly diminishing. As a result, many infrastructure projects are forced to be developed on weak or compressible soil deposits that exhibit poor load-bearing capacity and significant differential settlement potential[3–5]. These conditions can lead to severe structural distress, reduced service life, and increased maintenance costs, thereby affecting both public safety and national economic stability[6,7]. To address these challenges, geotechnical engineers have developed several soil stabilization and ground improvement techniques such as dynamic compaction, preloading with vertical drains, vacuum consolidation, chemical grouting, and soil reinforcement. Among these, the stone column technique stands out as one of the most reliable, cost-effective, and environmentally sustainable solutions, particularly for treating soft clayey or silty subgrades[8–11].

The stone column method involves the installation of compacted granular material into weak soils, creating a composite ground system that exhibits superior shear strength, stiffness, and drainage capacity. The inclusion of stone columns significantly improves the engineering behavior of soft soils by increasing their bearing capacity, reducing both total and differential settlements, accelerating consolidation, and enhancing resistance to liquefaction in loose saturated deposits[12–14]. The effectiveness of this method can be attributed to three primary mechanisms: (i) replacement of weak soil with dense granular material, which enhances composite stiffness and load distribution; (ii) radial drainage through the columns, which accelerates pore water dissipation and consolidation; and (iii) confinement effects that increase lateral earth pressure, densifying the surrounding soil and improving its strength[15–18]. However, the performance of stone columns strongly depends on the confining pressure of the surrounding soil. In very soft soils or layered profiles with low-stiffness top strata, insufficient confinement can lead to excessive lateral bulging near the column head, resulting in premature failure and reduced efficiency[6,19,20]. Previous research[21] has shown that stone columns can increase the load-bearing capability of poor soils by as much as ten times[22].

Department of Civil and Environmental Engineering, College of Engineering, Majmaah University, Majmaah 11952, Saudi Arabia. email: a.alaoni@mu.edu.sa

Field soils are often heterogeneous or stratified, comprising alternating layers of clay, silt, and sand with varying stiffness and permeability. Under such conditions, the load transfer mechanism and settlement behavior of reinforced ground become complex and require detailed investigation[4,23–25]. Recent research has advanced the understanding of stone column behavior through analytical, numerical, and experimental approaches. Studies have explored topics such as encased stone columns, dynamic and seismic performance, liquefaction resistance, and the use of recycled or alternative materials[8,26,27].

Numerous theories that take into consideration various failure mechanisms have been put forth to assess the bearing capacity and settling of stone column-reinforced ground. Recent advancements in estimating the bearing capacity and settlement of stone column–reinforced ground have incorporated sophisticated numerical modelling and experimental validations, focusing on geosynthetic encasement and seismic influences. For instance[28] examined the seismic behaviour of geosynthetic encased columns compared to ordinary stone columns, revealing enhanced resistance to dynamic loads through encasement while Das Das and Dey[29] proposed analytical frameworks that correlated column geometry and material properties with bearing capacity improvements. Other researchers have examined innovative fillers, such as rubber chips, recycled aggregates, and hybrid mixtures, which promote sustainability without compromising structural performance. Bahadori et al.[30] Rubber drainage columns were found to be helpful in lowering post-shaking settlements when liquefaction mitigation was compared to gravel. Chen et al.[31] examined the uniaxial compression behaviour of stone columns covered with geotextile, emphasising the reduced lateral deformation and enhanced rigidity. Tan and Zhao[32] used numerical simulations to examine the deformation and failure of isolated single stone columns with and without geosynthetic encasement. Ng[33] carried out a numerical analysis of the bearing capacity of single stone columns and found that the surrounding soil shear strength and the column friction angle had an impact on the failure modes of bulging and a combination of bulging and punching[34]. examined how the area ratio affected the pressure-settlement curves for circular footings using finite element analysis of geogrid-encased stone columns. El-Garhy et al.[35] examined flexible rafts on soft soil enhanced by granular piles using finite element methods, taking soil shear interactions into account. Zarazvand and Frankovska (2025) assessed the performance of stone columns in fine soil conditions using case studies for expressway embankments based on FEM[36,37]. Abdelhamid et al. (2025) evaluated floating encased stone columns experimentally on collapsible soils while taking reinforcing and recycled materials into account. For stone column-reinforced foundations, an optimised analysis approach based on the homogenization technique was suggested and verified using FEM and centrifuge testing[38].

Filz et al.[39] analysed settlement and vertical load transfer in column-supported embankments using 20 case histories, recommending design considerations for load distribution. Deshpande et al. (2021) conducted a case study on railway embankments supported by geosynthetic-encased stone columns in soft clays, focusing on settlement reduction. Naskar et al. (2024) used 3D finite element analysis to study stone column behaviour in layered soil with geosynthetic reinforced beds. A 2025 experimental study on bearing characteristics of stone columns in stratified transparent soil examined failure modes in sand-over-clay systems, revealing bulging localization in underlying clay layers[40].

Despite these advances, there remains limited research on the mechanical behavior of stone columns constructed with naturally available riverbed materials under realistic layered soil conditions.

In this context, the present study focuses on investigating the performance of stone columns constructed using riverbed gravel as an economical and sustainable alternative to conventional crushed stone aggregates[41]. The embodied energy of riverbed gravel is estimated to be 65–80% lower than that of quarried, mechanically crushed stone since it usually requires no crushing effort. Furthermore, regional cost figures show savings of 25–35%, which strengthens the case for using riverbed gravel as a sustainable substitute.

A series of laboratory model tests were conducted on floating stone columns embedded in both homogeneous and layered soil beds to evaluate their settlement response, axial load-bearing capacity, and bulging behavior under varying loading conditions. The findings from this experimental program provide valuable insights into the feasibility of utilizing riverbed gravel in ground improvement works, promoting cost-effective, sustainable, and locally adaptable solutions for infrastructure development in soft and stratified soils. Riverbed gravel, being naturally rounded and poorly interlocked compared to angular crushed aggregates, exhibits reduced shear resistance and a tendency for particle rearrangement, which leads to a distinct settlement pattern and failure mechanism.

Materials and methods

The materials utilized and several types of laboratory tests conducted to assess their basic physical characteristics are thoroughly described in this paper. It offers comprehensive instructions for preparing the soil bed and building stone columns. Moreover, describes the experimental configuration used to measure applied load, settlement behavior, and stone column failure types. The methodology is presented in Fig. 1.

Material

Sand

The river sand utilized during the present investigation was derived from natural deposits in the area. The sand's maximum and minimum dry densities, according to laboratory tests, were 17.2 kN/m³ and 14.6 kN/m³, respectively. In order to assess the shear and deformation properties of representative sand specimens, a series of drained triaxial compression tests were conducted in order to calculate the angle of internal friction and modulus of elasticity.

Clay

The fine-grained clay utilised in this study was collected locally, and bigger particles were then removed by sieving it using a 0.75 mm screen. Specific gravity = 2.7, liquid limit = 42%, plastic limit = 31%, optimal moisture

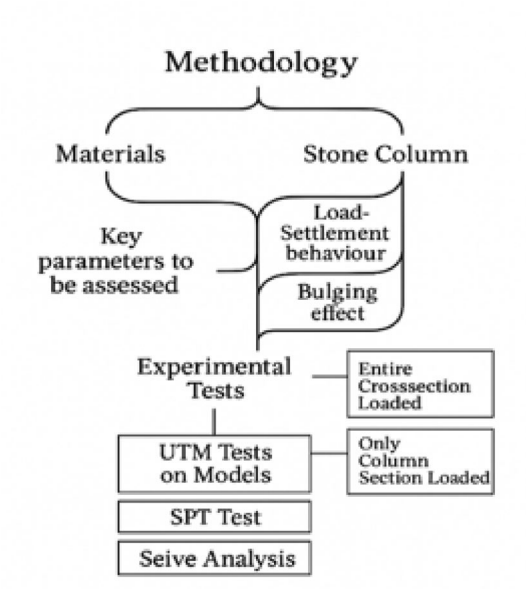

Fig. 1. Research methodology flowchart illustrating sequential stages of material characterization, model preparation, testing procedures, and data interpretation.

content = 21%, and maximum dry density = 16.6 kN/m^3 are the clay's primary physical characteristics. The material is categorised as CI–MI in accordance with the Indian Standard (IS) soil classification system.

In order to generate a range of consistencies, samples compacted at standard Proctor energy with different moisture contents were subjected to unconfined compressive strength (UCS) testing. Clay samples were made for the model testing programme with two different consistencies: stiff clay, which had an undrained shear strength of 54 kPa, and soft clay, which had an undrained shear strength of 15 kPa, which had a water content of 35%[34].

The results of one-dimensional consolidation tests were used to determine the modulus of elasticity for both soft and stiff clay conditions. The reciprocal of the coefficient of volume compressibility was used to calculate this modulus within the 100–200 kPa effective stress range. It is considered to be reasonable to use the constrained modulus derived from consolidation data since the stone columns serve to contain the surrounding clay. When evaluating the performance of internal stone columns inside column groups, this method accurately captures the stress-strain behaviour of the confined soil[35].

Stone column material

Coarse aggregate is defined as ground particles larger than 4.75 mm or retrained on a 4.75 mm screen, also known as screen No. 4. The aggregate used to construct a stone column might be observed between 2 and 10 mm in size. Grain size is achieved by passing aggregates through a sequence of sieves.

Riverbed gravel

Riverbed gravel, composed of stones, sand, silt, and clay shaped by flowing water (Fig. 2), varies in size and type depending on the river's geology and flow conditions[42]. In this study, gravel collected from a nearby riverbed was sieved to obtain coarse aggregates (2–10 mm) for use in stone column construction, offering a natural and economical filler material as depicted in Fig. 3. Riverbed gravel typically has smoother surfaces, rounded shapes, and better particle interlocking under load.

Methods

Laboratory test

The main objective of the laboratory studies was to assess the basic geotechnical properties of the aggregates and soils used in this experimental program. The obtained clayey soil's sieve analysis revealed that it falls into the AASHTO system's A-7-6 classification, which denotes subgrade material of low quality. The soil was classified as CI, or clay of intermediate plasticity, by the Unified soil classification system (USCS).

The clay was found to have a specific gravity of 2.52, which is in line with normal values for fine-grained soils. The results of the Standard Proctor compaction test showed that the maximum dry density (MDD) was 15.06 kN/m^3 and the optimum moisture content (OMC) was 13. According to these results, the clay's high compressibility and relatively low strength make it unsuitable for direct use as a foundation material in the absence of ground improvement techniques such reinforcing stone columns[37].

The silty soil sample, also collected locally, was found to be better graded compared to clay. Sieve analysis placed it under the SW category (well-graded silty sand) according to USCS, and A-2-7 under AASHTO classification. The particle size distribution showed coefficients of uniformity (Cu) and curvature (Cc) values of 4.13 and 1.02 respectively, confirming well-graded soil. Its specific gravity was determined as 2.67, which falls

Fig. 2. Laboratory soils employed in testing: (**a**) clay, (**b**) silt, and (**c**) sand samples after preparation.

Fig. 3. Stone column materials: (**a**) crushed coarse aggregates and (**b**) riverbed gravel obtained from local sources.

within the range for silt soils. This indicates a comparatively stable soil structure that could serve as a useful filler material[43].

The sand sample, on the other hand, was categorized as poorly graded sand (SP) under USCS with a fineness modulus (FM) of 2.56, which places it in the range of fine sand. The specific gravity of 2.63 further confirmed its sandy nature. Poorly graded sand typically has low cohesion and may require compaction or stabilization for structural use; however, its granular nature makes it suitable for use as backfill or drainage material.

For coarse aggregates, sieving confirmed particle sizes in the 2–10 mm range, with classification as poorly graded gravel (GP) under USCS. Specific gravity tests conducted in accordance with ASTM C127[44] showed an oven-dry value of 2.66, SSD (saturated surface dry) value of 2.69, and apparent specific gravity of 2.73. Water absorption was recorded as 1.03%, indicating a dense, strong material suitable for use in stone column construction and ground improvement. Los Angeles Abrasion tests showed values of 22% for crushed stone and 38% for riverbed gravel, indicating weaker particle resistance in gravel.

Model test

Model setup

The experimental setup for evaluating settlement and load behaviour was equipped with precise instruments and a well-prepared testing environment to ensure accuracy and reliability as depicted in Fig. 4. Settlement measurements were taken using a highly sensitive dial gauge with a 30 mm capacity and 0.01 mm accuracy, which allowed even the smallest displacements to be recorded. The load was applied using an electrically powered digital hydraulic compression machine with a maximum capacity of 20 tons. This machine was not only responsible for applying uniform and controlled loading through a hydraulic jack but also provided a real-time display of the applied load. Additionally, it generated a time–load graph, which was useful for determining the rate of loading and assessing the strength and durability of the tested material at various stages of loading. The soil and column specimens were placed inside a heavy-duty cylindrical steel testing tank, measuring 254 mm in diameter and 304.8 mm in height, with a wall thickness of 6 mm to resist deformation. The experimental setup consisted of a tank with an external diameter (De) of 254 mm and a column diameter (d) of 63 mm, resulting in

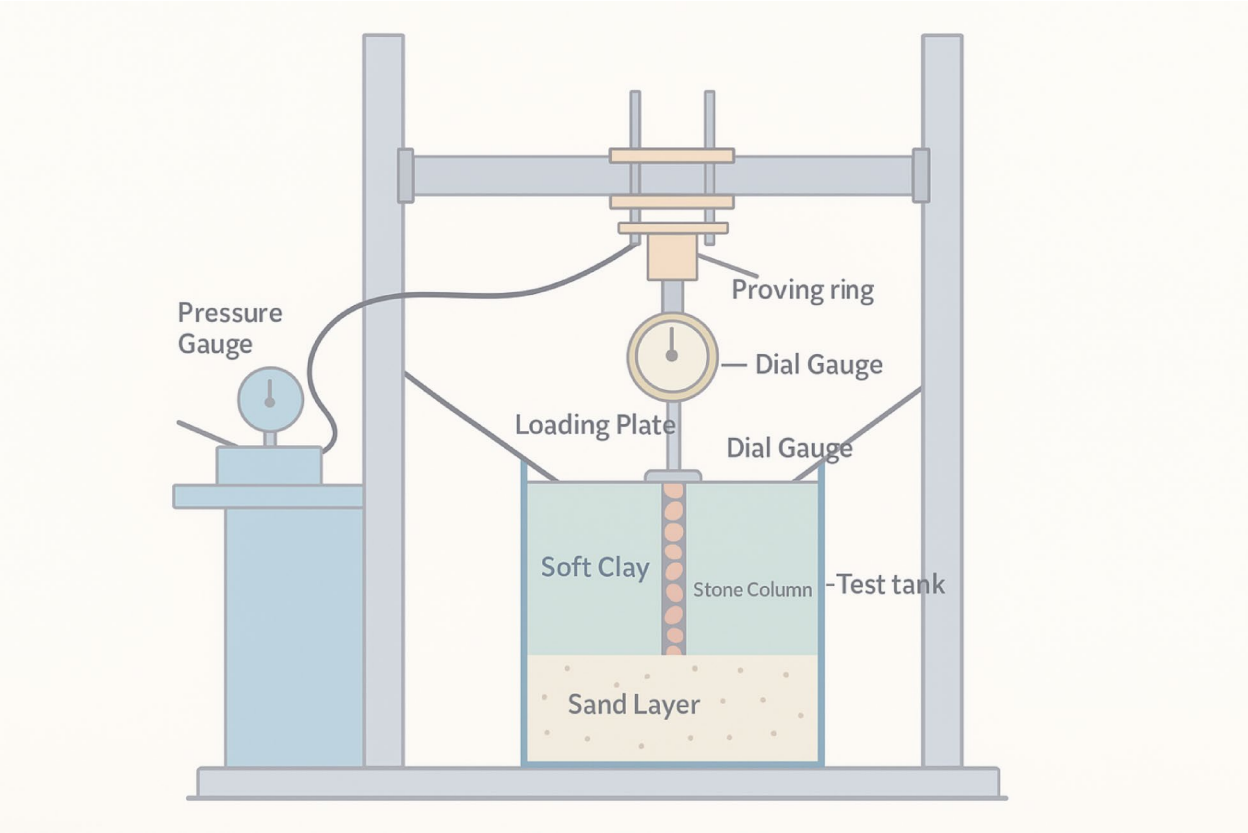

Fig. 4. Schematic illustration of the experimental setup showing load application system, test tank, and instrumentation.

a diameter ratio (De/d) of 4.03. The column length (L) was 250 mm, giving a length-to-diameter ratio (L/d) of 3.97. The tank had an open top and a closed bottom, ensuring confinement during testing, and it was filled with a carefully prepared three-layered soil bed to simulate field conditions. The soil profile included a compacted sandy layer of 63.5 mm at the base to provide drainage and stability, an intermediate silty layer of 101.6 mm to replicate natural stratification, and a top clayey layer of 127 mm to represent weak subsoil prone to settlement. To simulate different loading scenarios, two types of rigid steel plates were employed: one with a diameter of 252 and 10 mm thickness for loading the entire tank surface (including the stone column and surrounding soil), and another smaller plate with a diameter of 76.2 mm and thickness of 12.7 mm for loading only the surface of the stone column. These arrangements allowed comparison between uniform loading and concentrated loading conditions, thereby replicating real-world situations such as foundation settlement under distributed building loads or localized column loads. The loading was applied at a rate of 0.30–0.35 kN/s, which corresponded to a vertical platen movement of 0.6 mm/min. The test was terminated upon reaching either (i) a clearly identifiable peak load, or (ii) a settlement equal to 10% of the plate diameter, whichever condition occurred first. The combination of high-precision instruments, strong containment, layered soil simulation, and varied loading conditions ensured that the tests could accurately capture the settlement and strength characteristics of the soil–stone column system.

Formation of soil sample

The formation of soil samples was carried out with great care to ensure that the test conditions closely resembled real ground behaviour. Two types of soil sample preparations were considered: homogeneous soil beds and layered soil beds. In the homogeneous soil tests, only one type of soil was placed in the test tank—for example, if clay was selected, then the tank was filled entirely with clay, and similarly for sand. In contrast, the layered soil tests were designed to simulate natural stratification, where the soil profile was composed of three distinct layers: a top clay layer of 127 mm (5 inches), a middle silt layer of 101.6 mm (4 inches), and a bottom sand layer of 63.5 mm (2.5 inches), as illustrated in Fig. 4. The silt layer is roughly three times stiffer than the clay ($E_{clay}/E_{silt} = 0.333$); the sand is roughly 2.67 times stiffer than the silt ($E_{silt}/E_{sand} = 0.375$), and overall, the sand is nearly eight times stiffer than the clay ($E_{clay}/E_{sand} = 0.125$). This stiffness contrast between the layers demonstrates a progressive increase in modulus with depth. This suggests that the clay and sand layers are where the biggest stiffness transformation takes place.

Before soil placement, the steel tank was thoroughly cleaned with a cloth to remove dust or debris. The inner walls were coated with a thin layer of oil using a brush, after which a thin plastic sheet was fixed to the tank walls[24,36]. This arrangement acted as a friction-reducing layer, ensuring that the interaction between the soil and

tank wall did not interfere with settlement measurements; the oil also served as an adhesive for the plastic sheet. Once the tank was prepared, soil was added in layers, and each layer was compacted systematically. Compaction was performed by dropping a 1.5 kg rammer from a height of 100 mm (3.93 inches), delivering 20 uniform blows per layer. This method ensured consistent density and minimized voids within the soil mass.

After compaction, the prepared soil bed was covered with a plastic sheet and allowed to rest for 24 hours to facilitate uniform moisture distribution throughout the sample. This step was crucial, particularly for clayey and silty soils, as it allowed pore water pressures to stabilize before the application of load. Once the curing period was completed, the soil sample was transferred to the hydraulic compression machine. The loading plate was carefully placed over the soil surface or stone column (depending on the test), and a dial gauge was mounted to accurately measure settlement under applied loads[45].

To ensure accurate data collection, two mobile cameras were synchronized to start recording simultaneously during the test. These recordings captured the entire loading and settlement process, and data was extracted by pausing the videos at regular time intervals to record the displacement readings. This approach not only minimized manual observation errors but also provided a reliable means of cross-verifying the results. A pictorial view of the test procedure and soil formation steps is presented in Fig. 5. measuring 63.5 mm (2.5 inches).

Installation of floating stone column

The installation of the floating stone column was carried out using controlled procedures to ensure uniformity and reliability, as illustrated in Fig. 6. The process began with the preparation of a 50.8 mm (2-inch) compacted sandy base layer at the bottom of the tank. This layer served as both a drainage medium for pore pressure dissipation during loading and a firm foundation to anchor the stone column. A rubber pipe with an internal diameter of 63.5 mm (2.5 inches) and a wall thickness of 1 mm was then positioned vertically on the compacted base to act as a temporary casing, ensuring proper alignment and shape retention during construction. To facilitate smooth removal of the casing and to avoid disturbing the surrounding soil, its exterior surface was thoroughly greased using a brush.

Stone aggregates were placed inside the casing in three successive lifts, with each lift compacted using a 1 kg rammer dropped from a height of 80 mm. This light compaction energy was intentionally selected to densify the aggregates while minimizing stress transfer to the surrounding soil, which could otherwise induce premature lateral deformation during installation. After compaction, the casing was carefully withdrawn, leaving behind a well-formed, vertically aligned floating stone column embedded within the soil mass. The column remained "floating," meaning it did not extend to the rigid bottom boundary of the tank, thereby replicating typical field applications where stone columns are installed in weak soils without reaching a hard stratum. Such floating columns function by providing lateral confinement, redistributing stresses, and enhancing drainage, thereby improving the load-bearing and settlement characteristics of the treated ground. The sequential stages of installation are shown in Fig. 7.

To accurately capture the bulging deformation of the floating columns, a low-viscosity cement–water slurry was injected into the deformed column immediately after unloading to fill internal voids and preserve its bulged shape. The slurry was allowed to harden for 24 hours, after which the surrounding soil was carefully excavated in thin layers to expose the deformed profile. Measurements of the deformed diameter were taken at approximately 0.5D depth intervals using a digital Vernier caliper. The bulging percentage at each depth was calculated using:

$$\text{Bulging}\,(\%) = \left(\frac{D_{\text{deformed}} - D_0}{D_0}\right) \times 100$$

Program for experimentation

A comprehensive experimental program comprising a total of 20 laboratory tests, as summarized in Table 1, was carried out to investigate the settlement behaviour of soil reinforced with stone columns. All tests were conducted using a Hydraulic Compression Machine installed in the laboratory as shown in Fig. 8. The experimental program was divided into two categories based on the type of loading applied to the soil–column system. In the first category, the entire surface area of the tank, including both the soil bed and the stone column, was subjected to loading. In the second category, load was applied exclusively to the surface area of the stone column, thereby simulating localized foundation loading conditions. For these two loading conditions, different rigid steel plates were employed Loading Plates. This approach allowed a systematic evaluation of the response of

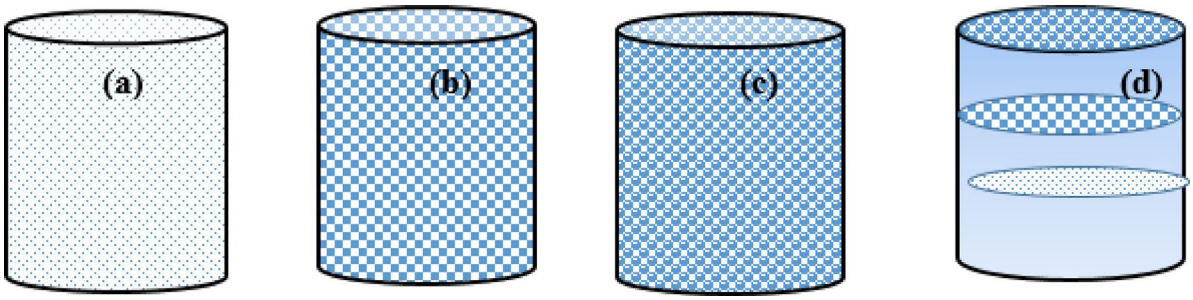

Fig. 5. Soil tank configurations prepared for testing: (**a**) clay, (**b**) silt, (**c**) sand, and (**d**) layered soil beds.

Fig. 6. Stepwise preparation of soil samples for model testing: (**a**) tank lubrication, (**b**) plastic sheet placement, (**c**) soil compaction, (**d**) prepared sample, (**e**) curing process, and (**f**) testing under hydraulic compression machine.

reinforced soil under both uniform and concentrated load applications, thereby providing a realistic simulation of varying field conditions.

Test matrix

The experimental program was systematically designed to cover both homogeneous and layered soil conditions, with a total of 20 tests conducted across different scenarios. For the homogeneous soil bed category, individual tests were performed on sand, silt, and clay, while in the layered soil bed category, a stratified profile of sand, silt, and clay was prepared. Each soil condition was tested under five distinct cases: (i) soil bed without reinforcement, (ii) soil bed reinforced with a stone column with load applied to the entire surface area, (iii) soil bed reinforced with a stone column with load applied only on the column surface, (iv) soil bed reinforced with an admixture stone column with load applied to the entire surface area, and (v) soil bed reinforced with an admixture stone column with load applied only on the column surface. For each of these conditions, one test was carried out on sand, silt, clay, and the layered soil bed, resulting in a total of 20 tests as summarized in (Fig. 9a). This systematic arrangement as depicted in Fig. 9b) allowed for direct comparison of settlement performance between reinforced and unreinforced conditions under varying soil types and loading conditions. In full-area loading, the applied load is distributed uniformly across the entire surface, resulting in an even stress distribution throughout the material. In contrast, column-only loading concentrates the load over a small area, producing high stress directly beneath the column that gradually spreads outward with depth. The schematic diagram clearly illustrates this difference, highlighting the uniform stress pattern under full-area loading versus the localized stress concentration and radial spreading in column-only loading.

Results and discussion

Load–settlement behavior of untreated soil beds

Four laboratory tests were conducted, each of which matched the type of soil that was placed into the test tank (Fig. 9). In the case of layered soil, the upper and lower strata were varied according to the intended configuration, whereas in the experimental setup, a soft clay layer was placed on top of a comparatively stronger

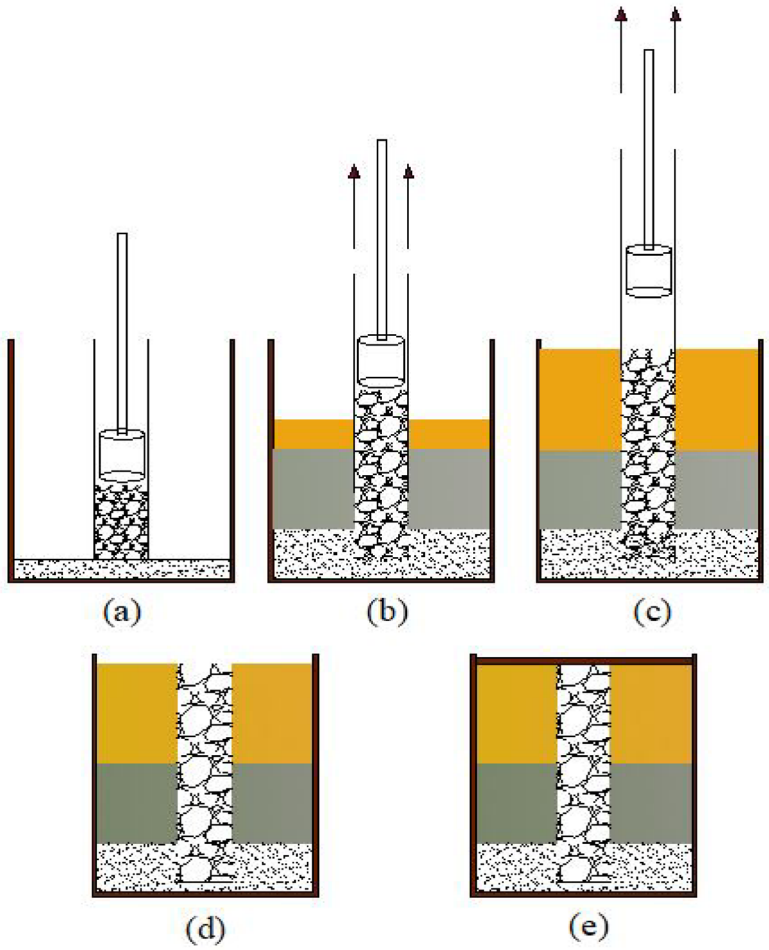

Fig. 7. Installation stages of floating stone columns: (**a**) sand base preparation, (**b**,**c**) aggregate placement and compaction, (**d**) completed column specimen, and (**e**) test setup with loading plate.

Parameter	Sandy soil	Silty soil	Layered soil	Clayey soil
Initial (0 mm)	Bulging = 1.35%, L/D = 0.00	Bulging = 4.94%, L/D = 0.00	Bulging = 11.84%, L/D = 0.00	Bulging = 6.57%, L/D = 0.00
Peak deformation	4.11% at L/D = 0.52	8.40% at L/D = 0.53	16.90% at L/D = 0.51	10.36% at L/D = 0.54
Mid-depth	Bulging = 0.88%, L/D = 0.99	Bulging = 4.16%, L/D = 0.96	Bulging = 10.77%, L/D = 1.06	Bulging = 4.99%, L/D = 1.04
Lower third	Bulging = 0.06%, L/D = 1.54	Bulging = 0.46%, L/D = 1.27	Bulging = 2.16%, L/D = 1.68	Bulging = 0.35%, L/D = 1.48
Base (L/D > 2)	Bulging < 0.15%, negligible variation	Bulging ≈ 0.03%, stable	Bulging ≈ 0.02%, stable	Bulging ≈ 0.01%, stable

Table 1. Bulging performance of coarse aggregate stone columns in different types of soil.

sandy layer, as explained in the sections above. Under low load levels (0–3 kN), it was found that all soil types showed essentially the same settlement reactions.

The existence of residual voids inside the compacted soil mass is responsible for this initial uniformity in deformation. A portion of the applied weight was used to remove these voids even though the compaction was done by hand with the greatest amount of effort. As a result, the initial loading phase was mostly linked to soil densification and compression, following which each kind of soil showed unique load-settlement behaviour.

Considering the tested soils differed in structural composition and particle size distribution, settlement characteristics varied significantly. The clayey soil, which is categorised as a soft soil, showed significant settlement, even under low loads. Its fine-grained structure, high water content, and increased compressibility all contribute to this reaction. The silty soil, which is also made up of small particles, showed the second-highest compressibility. It deformed noticeably under low load levels, albeit not as much as clay. The coarse-grained structure, low compressibility, and reduced void ratio of the sandy soil, on the other hand, allowed it to withstand higher loads with less settlement, resulting in superior load-bearing performance (Fig. 10).

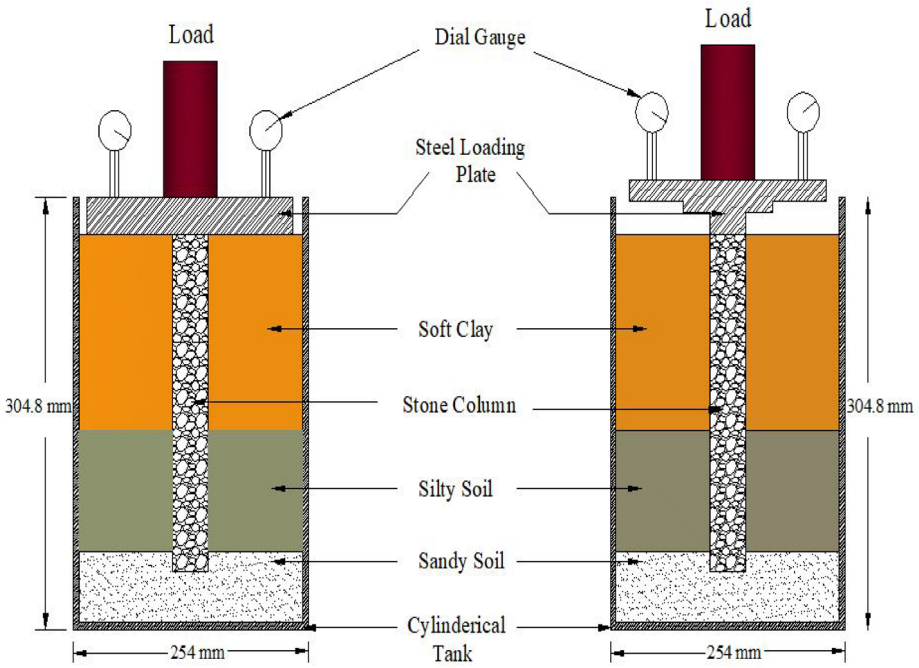

Fig. 8. Laboratory experimental setup showing hydraulic compression machine used for loading tests.

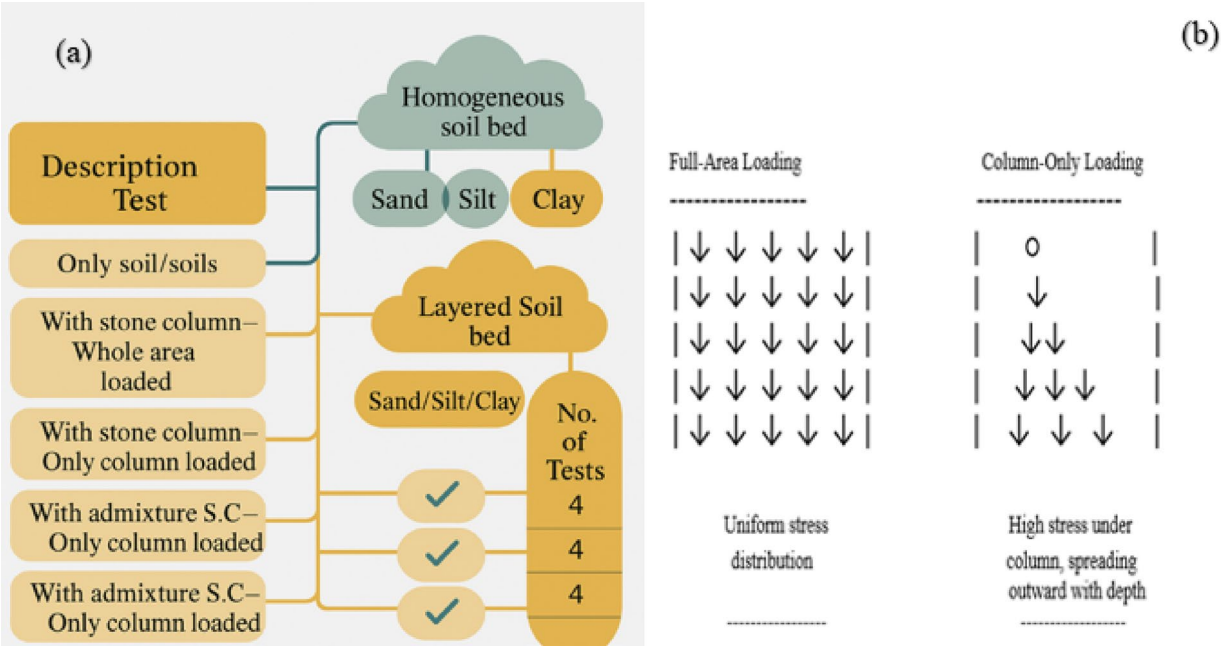

Fig. 9. (**a**) Test matrix illustrating the sequence of 20 model tests under varying soil and loading conditions (**b**) Comparison of stress distribution full area vs column loading.

An intermediate settlement response was displayed by the layered soil bed, which was composed of a base of compacted sand, an intermediate layer of silt, and a top layer of clay. The response was larger than that of pure sand but lower than that of clay and silt. The weaker upper layers (clay and silt) mostly affected the overall deformation of this layered system, but the underlying sand moderately improved stiffness and load-carrying capability. However, the composite system was less effective than the sandy soil alone since its mechanical behaviour was still controlled by the compressible upper layers.

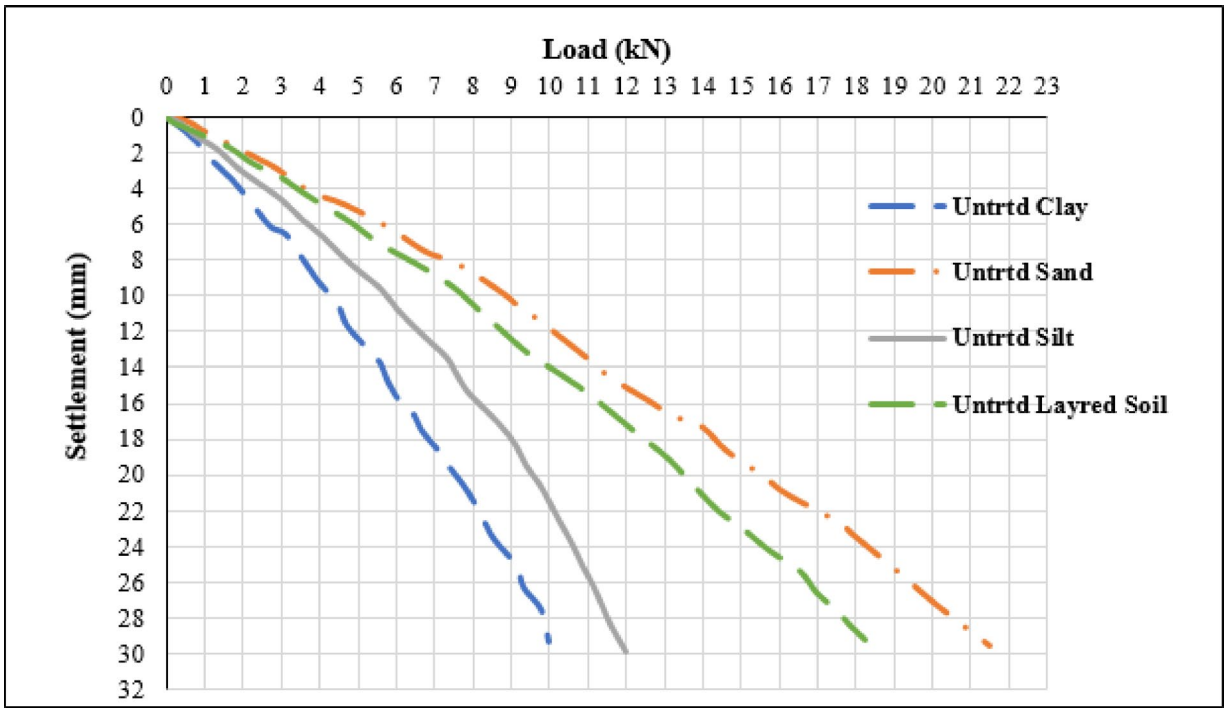

Fig. 10. Load–settlement response of untreated soil beds under applied loading conditions.

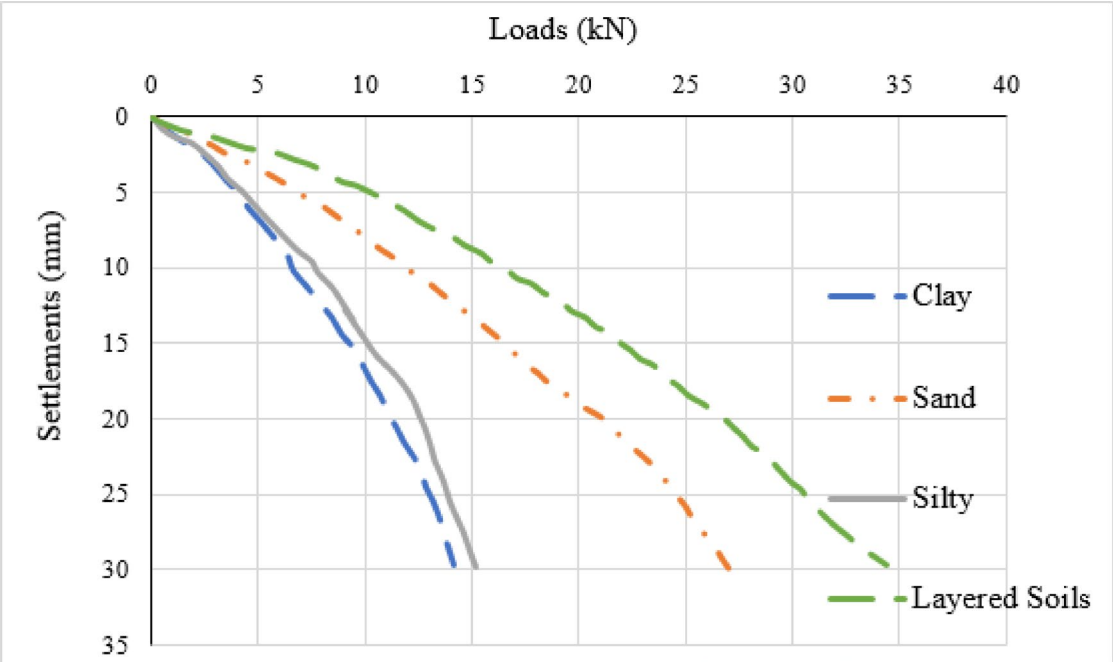

Fig. 11. Load–settlement curves of treated soils reinforced with stone columns under entire-area loading.

Performance of treated soil under entire-area loading

To enhance engineering qualities, stone columns were placed in the soil bed, which is referred to as treated soil. The performance of these reinforced soil systems under applied loading circumstances was assessed using four sets of laboratory tests. The experimental results from these tests are shown in Fig. 11, together with the accompanying graphical representations.

Although the amount of improvement varied depending on the intrinsic properties of each soil, the addition of stone columns significantly increased the load-bearing capacity across all soil types tested. Even at relatively

light loads, the untreated examples showed notable settlements in clayey soil, which is generally weak and highly compressible. However, the settlement was significantly lessened following the erection of stone columns. The stiffness difference between the surrounding soft soil and the compacted coarse aggregate columns is responsible for this improvement, since it allowed load transfer through both skin and end-bearing friction processes. Consequently, a significant amount of the applied stress was supported by the stone columns instead of the surrounding soil, which decreased total deformation and increased the treated ground's composite carrying capacity.

Similarly, silty soil, though softer and more compressible than sand, exhibited noticeable improvement when reinforced with stone columns, but the gain was limited because the column occupied a relatively small cross-sectional area compared to the tank, restricting its overall contribution. In contrast, sandy soil, already strong and less compressible, responded most favourably, with stone columns further increasing capacity due to strong interparticle friction and compatibility between coarse aggregates and sandy grains. The layered soil system—comprising clay at the top, silt in the middle, and sand at the bottom—displayed the most remarkable performance with stone column reinforcement. The clay allowed slight lateral expansion of the column, creating a wedge effect that restricted settlement, while the sandy base provided firm support, enabling both the soil mass and stone column to share the applied loads effectively. Overall, results demonstrated that stone column efficiency is strongly influenced by soil type, with the highest improvement observed in layered deposits, as illustrated in Fig. 11.

Load–settlement response of treated soil under column-only loading

The stone column was loaded according to illustrated testing setup, and the resulting data was recorded for analysis. The stone column significantly increased the composite system's load-carrying capability even though its cross-sectional area was limited as compared to the total soil mass. The column could withstand larger loads than the system tested under full area loading circumstances because it was made of coarse aggregates that were densely compacted. It also showed a noticeably stronger resistance to deformation.

The distribution of applied stress explains the variation in load-bearing behaviour between the two testing methodologies. When whole area loading was used, the pressure was distributed throughout the whole cross-section of the soil mass, of which the stone column made up a very small portion. As a result, it made a relatively small contribution to the total bearing capacity. On the other hand, the stone column itself became the main load-bearing component when the load was applied straight across the column's cross-sectional area. Skin friction along the column–soil contact and end-bearing resistance at the column base were the main mechanisms for load transfer.

Under the same applied loads, the stone column showed noticeably less settlement because of its high degree of compaction and the confinement that the surrounding soil supplied. This behaviour, which is depicted in Fig. 12, demonstrates the column's superior performance when loaded separately and validates its ability to successfully improve the load-bearing properties of weak soils by means of localised reinforcement.

When loaded directly on the stone column, all soil types demonstrated improved performance, with varying degrees of enhancement depending on their inherent properties. In clayey soil, the small particle size facilitated strong skin friction between the soil and the stone column surface, enabling a good bond and resulting in a notable increase in bearing capacity as shown in Fig. 13. Similarly, silty soil exhibited improved load resistance under column loading due to the same skin friction mechanism, though its response remained somewhat limited compared to sandy deposits. Sandy soil, being inherently strong and less compressible, showed remarkable load-carrying performance when reinforced with stone columns, confirming that stronger soils exhibit even greater improvement under column installation compared to weaker soils. Layered soil presented the highest increase in load-bearing capacity under this testing configuration; with the column directly loaded, settlements remained minimal even under large loads. This is attributed to the rigid, non-compressible nature of the stone aggregates that transferred a significant portion of the applied load to the surrounding soil, while additional resistance was mobilized through skin friction between the stone column surface and adjacent soil layers.

Load–settlement behavior of treated soil reinforced with riverbed gravel (entire-area loading)

For the purpose to assess their impact on load-settlement characteristics, stone columns made of riverbed gravel were positioned into the soil bed during this testing phase. In order to examine the impact of column material composition on the overall performance of the treated ground, natural riverbed gravel was substituted for typical crushed aggregates. At successive loading intervals, settlements were systematically measured, and the resulting data were documented for analysis. In order to illustrate the relative improvement in load-bearing behaviour brought about by the addition of riverbed gravel stone columns, the test results were then processed and visually depicted, as shown in Fig. 14.

The results indicated that soil reinforced with stone columns using alternative materials exhibited improved load-bearing performance, though not to the same extent as traditional stone aggregate columns, as illustrated in Fig. 14. When riverbed gravel was used as the column material, the soil response under loading showed higher settlements compared to conventional stone columns, primarily due to the relatively compressible nature of riverbed gravel, which can undergo crushing under applied stresses. In silty soil, the behavior was consistent with earlier trends, demonstrating better performance than clayey soil but remaining weaker than sandy deposits, with improvements still less pronounced compared to columns constructed with coarse stone aggregate. Sandy soil, already characterized by its strong load-bearing capacity, showed additional enhancement with column installation; however, the improvement with riverbed gravel columns was again lower than that achieved with traditional stone aggregates. Layered soil once more outperformed the other soil types under this testing scheme,

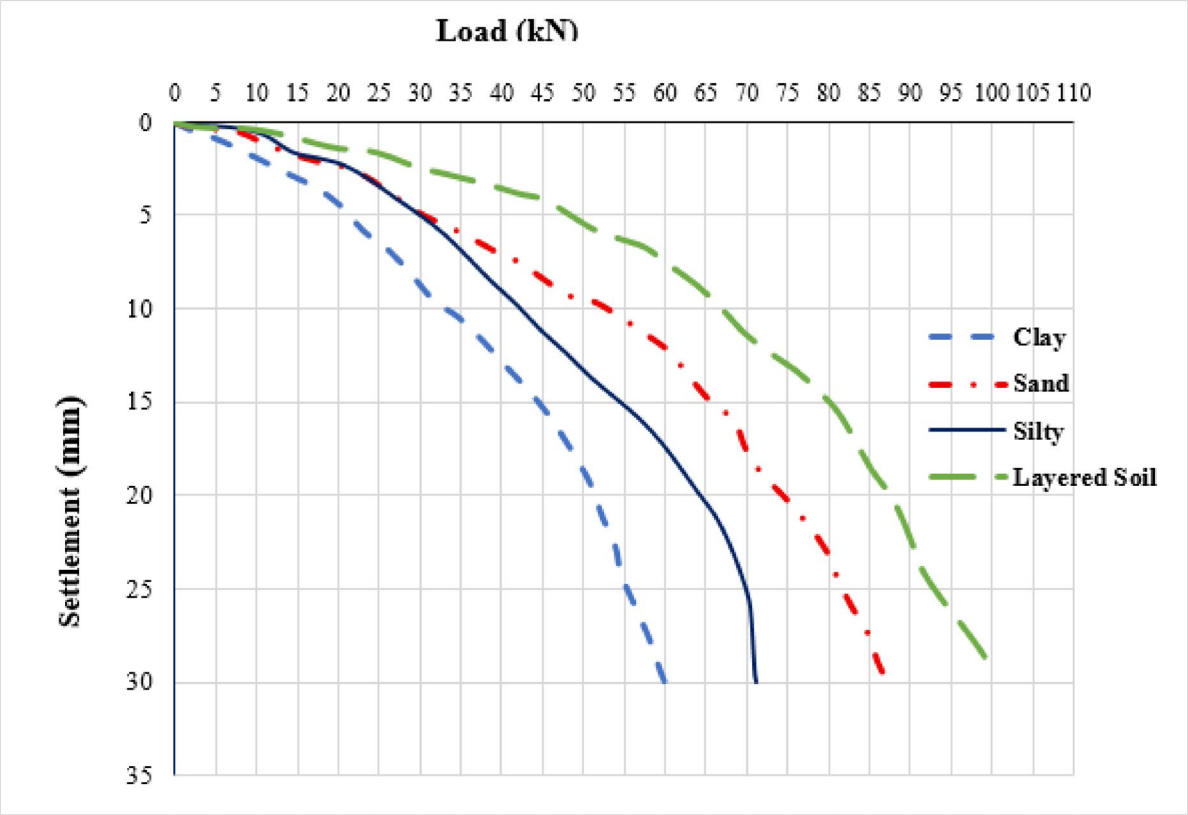

Fig. 12. Load–settlement behavior of treated soils when only the stone column area is subjected to loading.

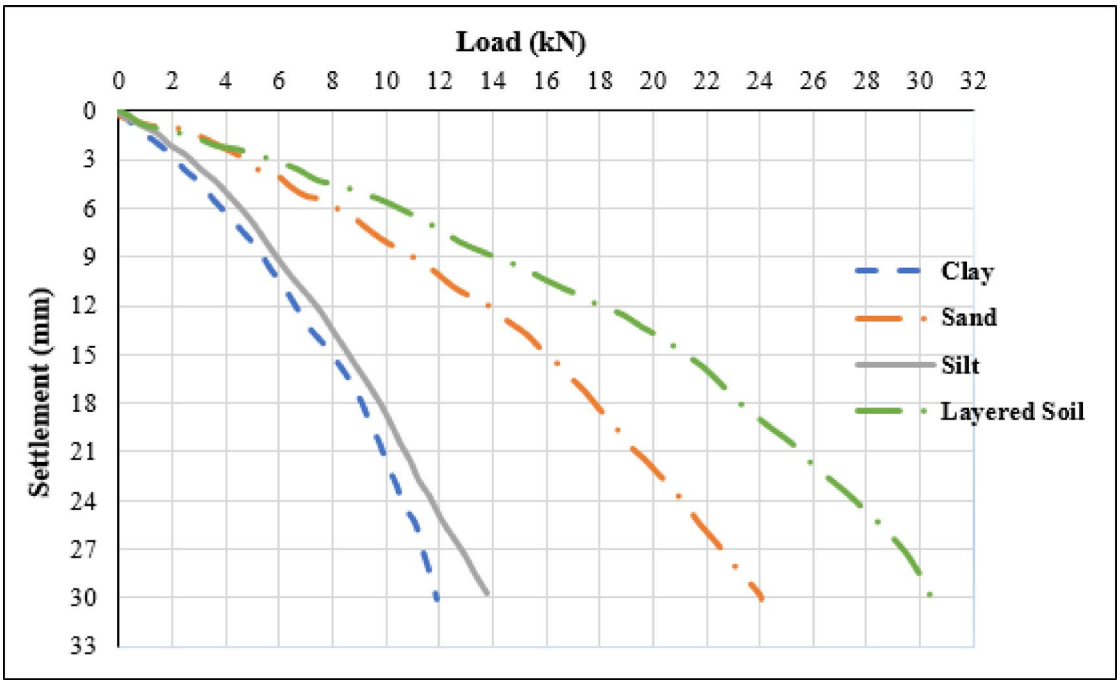

Fig. 13. Load–settlement curves of riverbed gravel stone columns subjected to localized (column-only) loading.

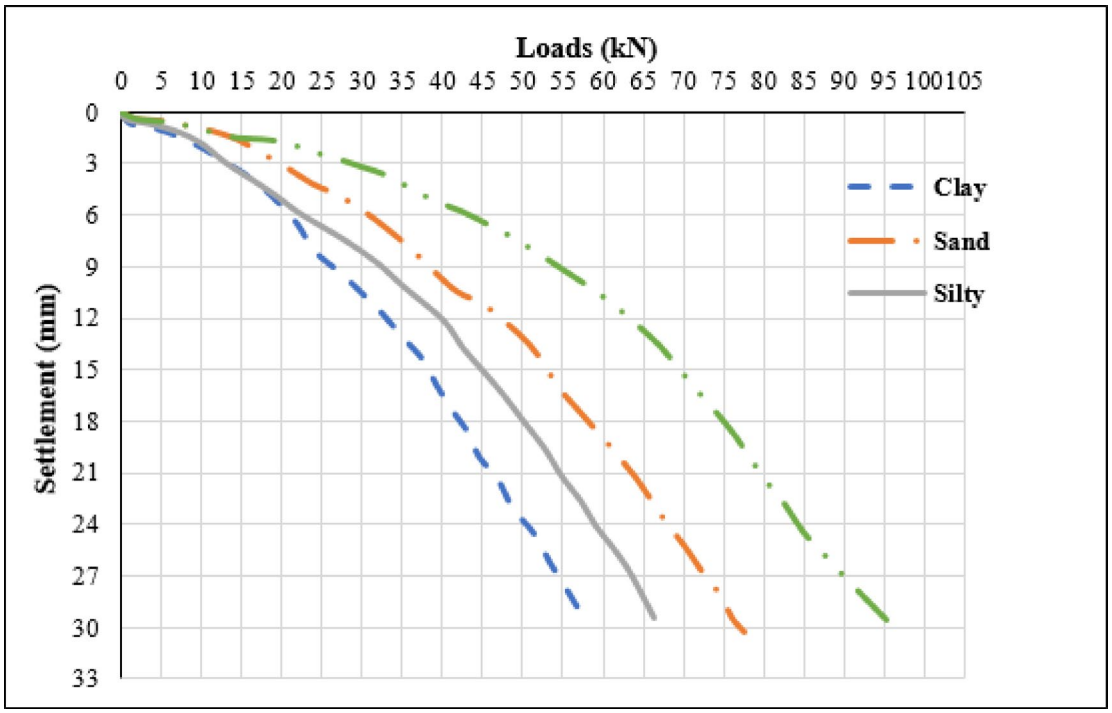

Fig. 14. Comparative load–settlement performance of soils reinforced with riverbed gravel stone columns under full-area loading.

benefitting from the combined soil–column interaction, though even here the bearing capacity remained higher with conventional stone columns compared to those formed with compressible gravel.

Load–settlement behavior of riverbed gravel stone columns under column-only loading

In this test setup, the applied load was only focused on the stone column's cross-sectional area. In this instance, the stone column was made of riverbed gravel. For comparative analysis, similar tests were previously conducted with coarse aggregate columns. The coarse aggregate columns were found to have a higher load-carrying capability than the riverbed gravel columns, according to the results shown in Fig. 13.

The material strength and crushing resistance of the aggregates utilised are responsible for this performance discrepancy. Because riverbed gravel is less angular and comparatively softer than coarse aggregate, it is more likely to compress under heavier loads. Particles are crushed under load, which reduces internal voids and causes more settlement in the test findings.

The type of soil in the area also affected how well the stone columns supported loads. Because clayey soil has a weak structure and a high compressibility, the columns showed significant settlement even under moderate loads. Larger deformations resulted from the column's propensity to sink or shift more easily within the soft clay matrix. However, the columns supported greater loads with relatively less settlement in silty soil. Its intermediate stiffness and increased shear strength, which improved confinement and decreased downward displacement, are responsible for the silt's improved performance.

Even under relatively heavy loads, the stone columns performed effectively when tested in sandy soil, which is composed of course and denser particles. In addition to improving end-bearing resistance and skin friction, the deep sand matrix provided significant lateral confinement. Overall, the behaviour was optimal when the soil was stratified and had silty, sandy, and clayey layers.

In order to create a wedge-like resistance that reduced column penetration, the clayey upper layer contributed restricted bulging, the silty intermediate layer improved load transfer through skin friction, and the sandy base layer offered strong support at the bottom. In contrast to any one soil type, including pure sand, the layered system incorporated the advantageous qualities of all three soils, producing superior load-bearing capacity.

Bulging behavior of floating stone columns

Bulging deformation of the floating stone columns was examined primarily under column-only loading, where the applied stress was concentrated directly on the column head. Immediately after unloading, a low-viscosity cement–water slurry was injected into the deformed column to preserve its distorted geometry, and the slurry was allowed to harden for 24 h. Once cured, the surrounding soil was carefully excavated to expose the bulged profile, and deformed diameters were measured at successive depths from the column head.

Across the different soil beds tested—sand, silt, clay, and layered configurations, distinct bulging behaviors were observed under the two loading conditions. When the entire tank surface was loaded, lateral deformation was minimal because applied stresses were shared with the surrounding soil, increasing passive confinement.

In contrast, column-only loading produced significantly greater bulging, particularly in homogeneous clay or silt beds, where weak confinement allowed lateral expansion. This trend aligns with previous findings[9], which reported maximum bulging at depths of approximately 0.5–0.8 times the column diameter.

In layered soil systems, bulging was concentrated within the upper clay layer, while the underlying stiffer silt and sand layers provided enhanced confinement. Consequently, full-area loading resulted in much lower deformation, whereas column-only loading reduced lateral restraint and caused more pronounced expansion near the surface. The investigation considered two types of column materials including coarse aggregates and riverbed gravel to capture the distinct deformation patterns associated with their mechanical characteristics, and the bulging performance of each material is presented separately in subsequent sections.

Bulging behavior of stone columns constructed with coarse aggregate

The bulging patterns of stone columns made of coarse aggregate were meticulously observed and examined after they were placed in a variety of soil types. Figure 15 is a graphic representation of the corresponding data. When compared to those in uniform sandy, silty, or clayey soils, the findings showed that the stone columns embedded in layered soil had the greatest degree of lateral deformation. The layered soil's compositional variability, which included a soft clayey upper layer and a dense sandy base layer, is responsible for this behaviour. There was noticeable bulging close to the top part because, under localised strain, the column expanded laterally into the weaker clay layer instead of piercing the dense sand layer underneath.

Stone columns embedded in pure clayey soil, on the other hand, exhibited comparatively less obvious bulging. Instead of expanding laterally under strain, the columns descended vertically due to the high compressibility and weak nature of clay. As a result, the column's upper section experienced the most deformation, while the lower part settled since there was insufficient bearing support.

According to an analysis of the test findings, the surrounding soil's compressibility and weakness increased the amount of bulging. Differential confinement circumstances caused the greatest deformation in the layered soil, which combined stiff and weak layers. This behaviour emphasises how important material stiffness and soil layering are in regulating the lateral deformation properties of stone columns under localised loading. Coarse aggregate columns displayed the greatest bulging in layered soil (≈ 16.9%) and the lowest in sandy soil (≈ 4.1%). The deformation decreased progressively with depth, stabilizing below L/D ≈ 2.0.

Bulging behavior of stone columns constructed with riverbed gravel

The results of an evaluation of the bulging performance of stone columns made of riverbed gravel as the column material are compiled in Table 2. According to the findings, columns made of riverbed gravel demonstrated more lateral displacement than those made of coarse particles. The mechanical properties of riverbed gravel, which are often smoother, less angular, and more prone to particle crushing under higher stresses, are largely responsible for this increased bulging reaction. Higher bulging deformation results from the material spreading laterally into the surrounding soil due to the reduced internal resistance caused by crushing these particles.

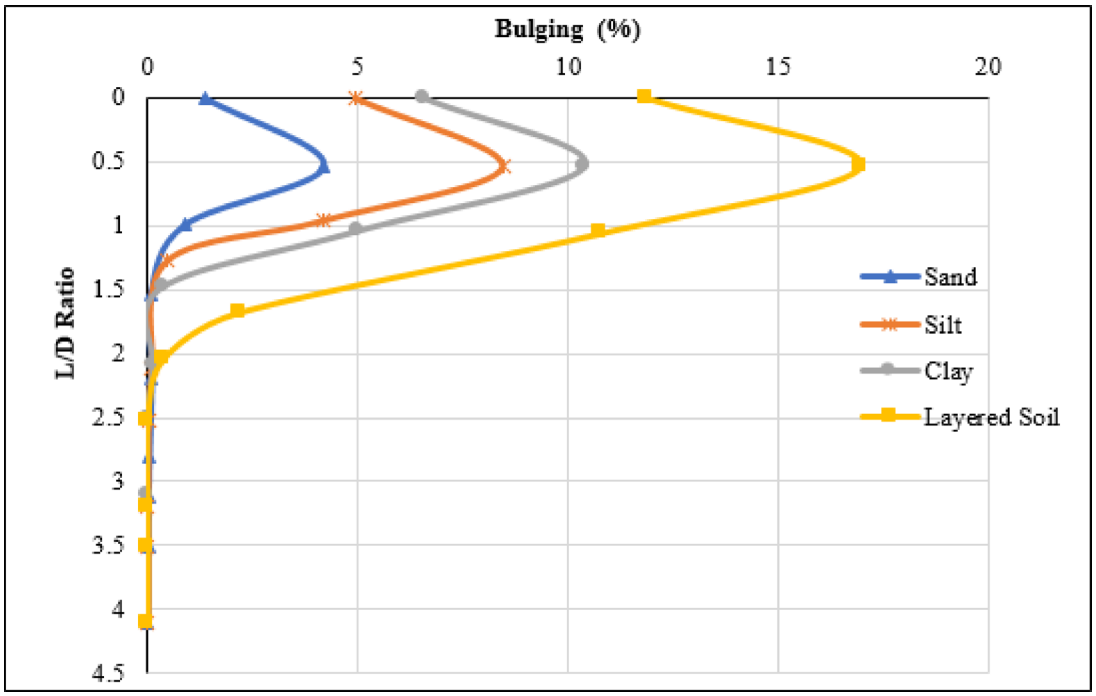

Fig. 15. Bulging profile and deformation pattern of coarse aggregate stone columns in various types of soil.

Parameter	Sandy soil	Silty soil	Layered soil	Clayey soil
Initial (0 mm)	Bulging = 2.51%, L/D = 0.00	Bulging = 6.55%, L/D = 0.00	Bulging = 12.88%, L/D = 0.00	Bulging = 9.26%, L/D = 0.00
Peak deformation	7.23% at L/D = 0.53	9.99% at L/D = 0.50	20.08% at L/D = 0.51	15.37% at L/D = 0.55
Mid-depth	Bulging = 4.13%, L/D = 0.94	Bulging = 5.49%, L/D = 0.98	Bulging = 10.79%, L/D = 1.04	Bulging = 8.88%, L/D = 1.18
Lower third	Bulging = 0.44%, L/D = 1.23	Bulging = 0.39%, L/D = 1.37	Bulging = 2.14%, L/D = 1.68	Bulging = 2.14%, L/D = 1.68
Base (L/D > 2)	Bulging < 0.10%, stable	Bulging ≈ 0.13%, stable	Bulging ≈ 0.03%, stable	Bulging ≈ 0.00%, stable

Table 2. Bulging characteristics of riverbed gravel (C.W) stone columns in different types of soil.

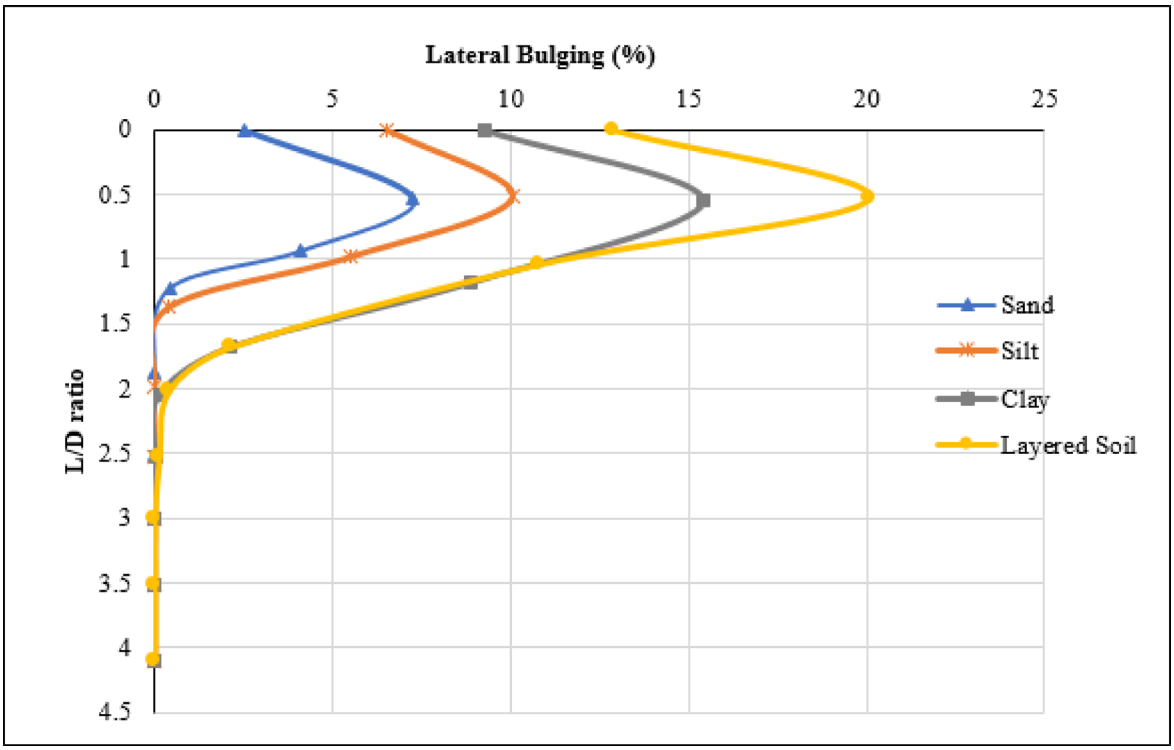

Fig. 16. Bulging behavior of riverbed gravel stone columns in different soil conditions.

On the other hand, stone columns made of coarse aggregates showed less bulging because each particle is stronger and more angular, which enables it to support more loads without being severely crushed. Consequently, these columns were better able to hold their shape, which prevented excessive lateral expansion.

Overall, the bulging behaviour trend across the various soil types remained in line with exactly what was shown in the earlier testing. Since the column material was the primary variable changed in this set of trials, variations in the degree of deformation were mostly controlled by the confinement conditions and mechanical characteristics of the surrounding soil. The results' matching graphical representation, which compares the riverbed gravel columns' performance under various soil conditions, is displayed in Fig. 16. Riverbed gravel columns exhibited higher surface bulging than coarse aggregate columns across all soil types. The maximum deformation occurred near the upper 0.5 D depth, particularly within layered and clayey soils, reflecting the greater compressibility and crushability of gravel materials[46].

The overall strength behavior of the stone columns seems to be influenced by the observed anisotropy. The material may be better able to withstand loading along specific orientations due to directional dependency[47] When the direction of stress changes, this non-uniform structure may cause minor variations in compressive and shear strength. The performance of soil under intricate field loading conditions may be impacted in practice by such anisotropic behavior[48,49].

Stress concentration around columns

An area of the tank that would typically support a load is removed when a column passes through a tank or plate. Resultantly, there is a concentration of stress around the column. While the load is now forced through a smaller region, the stress in the surrounding material is greater than the nominal stress. The area-replacement ratio quantifies how much of the total area is blocked by the column is calculated by the Eq. (1). Larger area replacement-ration column occupies more area, stress distribution is more uniform vice versa.

$$a_r = \left(\frac{d}{De}\right)^2 = 6.15\% \tag{1}$$

The nominal stress without a column is the stress near the column that can be approximated using the inverse area ratio as shown in Eq. (2).

$$\delta_{local} \approx \delta_0 . \frac{1}{a_r} = 16.25 \tag{2}$$

This indicates the stress surrounding the column is about 16 times higher than the nominal stress in that area. This is because the column blocks 6.15% of the cross-sectional area.

Conclusions

The load-bearing behaviour of different soil types reinforced with stone columns was examined through a thorough series of small-scale laboratory experiments. The study's main objectives were to compare the performance of stone aggregate and riverbed gravel as column materials and to examine the effects of stone columns built in clayey, silty, sandy, and layered soils. In order to evaluate their respective effects on settlement and bearing performance, the soil type, loading configuration, and column material were changed during the testing programme, while the columns' diameter, length, and strength remained unchanged. The performance of layered soil compared to pure sand is due to the combined effects of strength and confinement provided by alternating layers, which enhance load distribution and reduce deformation.

The findings clearly showed that adding stone columns greatly enhanced the load-bearing response of all soil types, with the degree of improvement varying according to the column material and soil properties. on comparison to the untreated state, the installation of riverbed gravel columns and stone aggregate increased the load-carrying capacity by 17.25 and 43.3%, respectively, when the full tank area was loaded on clayey soil. Improvements of 16.81% (riverbed gravel) and 25.42% (stone aggregate) were noted in silty soil. The two materials' respective increases in load-bearing capability for sandy soil were 27.03 and 13.32%. For stone aggregate and riverbed gravel columns, the overall bearing capacity in layered soil increased by 33.81% and 28.98%, respectively.

These results demonstrate how well stone columns support weak subsoils, especially when coarse aggregates are utilised as the column material.

Significant increases in maximum load-carrying capacity have been observed under axial loading conditions. Columns made of riverbed gravel and stone aggregate supported total loads of 58.02 kN and 61.06 kN, respectively, at about 30 mm settling on clayey soil. The highest axial loads for silty soil were 67.26 kN for riverbed gravel and 72.07 kN for stone aggregate. The corresponding values in sandy soil were 78.53 kN and 88.46 kN. The most effective performance was shown by the layered soil, which supported 101.35 kN and 96.38 kN when reinforced with riverbed gravel columns and stone aggregate, respectively. These findings demonstrate that both materials greatly increase load resistance; nevertheless, because of their greater angularity and crushing resistance, stone aggregate columns continuously perform better than riverbed gravel columns.

Although riverbed gravel is more susceptible to particle crushing under load, it showed more lateral deformation than stone aggregate columns, according to an analysis of bulging behaviour. The following were the maximum bulging values that were noted: At L/D ratios of 0.53 and 0.55, respectively, riverbed gravel made up 15.37% and stone aggregate made up 10.36% of clayey soil. 9.99% (riverbed gravel) and 8.40% (stone aggregate) with L/D ratios of 0.50 and 0.53, respectively, in silty soil. At L/D ratios of 0.51 and 0.43, respectively, 4.11% (stone aggregate) and 7.23% (riverbed gravel) were found in sandy soil. At an L/D ratio of 0.51 in layered soil, riverbed gravel makes up 20.08% and stone aggregate 16.90%. The riverbed gravel columns exhibited 80–95% of the bearing capacity and 70–85% of the stiffness compared to crushed stone columns.

In short, the findings support the assumption that bulging is more noticeable in weaker soils and when the column material is riverbed gravel. On the other hand, stone aggregate columns demonstrated better structural integrity and confinement, which made them more useful for enhancing the stability of weak subgrades.

Data availability

The data that support the findings of this study are available from the corresponding authors upon reasonable request.

Received: 13 October 2025; Accepted: 23 December 2025
Published online: 03 January 2026

References

1. Baqir, H. H., Aswad, M. F. & Fattah, M. Y. A numerical study on the behavior of stone columns with different area ratios in soft clays. *Geomate J.* **26** (117), 43–51 (2024).
2. Kumar, N. & Kumar, R. Performance of geosynthetic-encased stone columns in sandy soils subjected to vertical Cyclic loads. *Int. J. Geomech.* **25** (1), 04024323 (2025).
3. Abid, M. S. et al. Shear strength of geosynthetic-encased stone columns in unsaturated soils. *Geotech. Geol. Eng.* **42** (7), 6051–6070 (2024).
4. Foda, T. et al. Innovative approaches to soft clay stabilization: utilizing sustainable materials for the stone column technique. *Geotech. Geol. Eng.* **42** (6), 5143–5167 (2024).
5. Kumar, N. et al. Numerical analysis of a Dual-Layer Geosynthetic-Encased stone column installed in soft soil. *Adv. Civil Eng.* **2023** (1), 5039439 (2023).

6. Choobbasti, A., Zahmatkesh, A. & Noorzad, R. Performance of stone columns in soft clay: numerical evaluation. *Geotech. Geol. Eng.* **29** (5), 675–684 (2011).
7. Foda, T., Abdelkader, A. & Ibrahim, H. M. A review of soil stabilization using stone columns technique. *Delta Univ. Sci. J.* **6** (1), 39–50 (2023).
8. Fattah, M. Y., Al-Jamaily, N. M. & Salman, F. Improvement of the behaviour of embankment on soft soil by stone columns. In *Proceedings of the International Conference on Ground Improvement and Ground Control*. (eds B. Indraratna, C. Rujikiatkamjorn and JS Vinod) (2012).
9. Maghvan, S. V., Imam, R. & McCartney, J. S. Physical modeling of stone columns in unsaturated soil deposits. *Geotech. Test. J.* **43** (1), 253–274 (2020).
10. Abdelbaset, A. & Arafa, I. T. Improvement of consolidation settlement beneath square footings using uncased and encased stone columns. In *Structures*. (Elsevier, 2023).
11. Shukla, A., Kumar, R. & Kumar, N. Optimization of stone column performance using waste rubber crumbs and construction and demolition aggregate combination. p. 1–7 (National Academy Science Letters, 2025).
12. Shivashankar, R. et al. Experimental studies on behaviour of stone columns in layered soils. *Geotech. Geol. Eng.* **29** (5), 749–757 (2011).
13. McCabe, B. A., Nimmons, G. J. & Egan, D. A review of field performance of stone columns in soft soils. In *Proceedings of the Institution of Civil Engineers-Geotechnical Engineering*. **16** 2 (6), 323–334. (2009).
14. Krishnan, M. & GuhaRay, A. Evaluation of recycled construction and demolition waste as fillers in group of stone columns. *GEOVADIS* 123. (2025).
15. Mohanty, P. & Samanta, M. Experimental and numerical studies on response of the stone column in layered soil. *Int. J. Geosynthetics Ground Eng.* **1** (3), 1–14 (2015).
16. Han, J. & Ye, S. L. Simplified method for consolidation rate of stone column reinforced foundations. *J. Geotech. GeoEnviron. Eng.* **127** (7), 597–603 (2001).
17. Mohamed, M. Behaviour of encased stone columns in soft clay. *J. Eng. Res.* (2022).
18. Jaiswal, A. et al. *Influence of Dual Layer Confinement of Stone Column Material on the Shear Modulus of the Soil-Column Combined System* p. 1–8 (National Academy Science Letters, 2024).
19. Elshazly, H., Hafez, D. & Mossaad, M. Reliability of conventional settlement evaluation for circular foundations on stone columns. *Geotech. Geol. Eng.* **26** (3), 323–334 (2008).
20. Guetif, Z., Bouassida, M. & Debats, J. Improved soft clay characteristics due to stone column installation. *Comput. Geotech.* **34** (2), 104–111 (2007).
21. Priebe, H. J. The design of vibro replacement. *Ground Eng.* **28** (10), 31 (1995).
22. Dutta, R. K. et al. Performance of square footing resting on clay reinforced with granular columns. *Transp. Infrastructure Geotechnology*. **12** (6), 189 (2025).
23. Greenwood, D. Mechanical improvement of soils below ground surface. In *Inst Civil Engineers Proc.*. (1970).
24. Saxena, S. et al. Model tests on ordinary and geosynthetic encased stone columns with recycled aggregates as filler material. *Int. J. Geo-Engineering*. **15** (1), 1 (2024).
25. Alam, P. & Bawa, S. Sustainable use of waste materials in stone columns: a review. *Indian Geotech. J.* **55** (2), 1279–1300 (2025).
26. Daya Dath, N. A. Study on conventional aggregate and gravel as columnar inclusions In clay. In *International Conference on Geotechniques for Infrastructure Projects*. (2017).
27. Gupta, A. A review article on construction, parametric study and settlement behavior of stone column. In *IOP Conference Series: Earth and Environmental Science*. (IOP Publishing, 2021).
28. Cengiz, C. & Güler, E. Seismic behavior of geosynthetic encased columns and ordinary stone columns. *Geotext. Geomembr.* **46** (1), 40–51 (2018).
29. Das, M. & Dey, A. K. Improvement of bearing capacity of stone columns: an analytical study. In *Ground Improvement and Reinforced Soil Structures: Proceedings of Indian Geotechnical Conference 2020 Volume 2*. (Springer, 2021).
30. Bahadori, H. et al. A comparative study between gravel and rubber drainage columns for mitigation of liquefaction hazards. *J. Rock Mech. Geotech. Eng.* **10** (5), 924–934 (2018).
31. Chen, J. F. et al. Uniaxial compression behavior of geotextile encased stone columns. *Geotext. Geomembr.* **46** (3), 277–283 (2018).
32. Tan, X. & Zhao, M. Deformation and failure behavior of the isolated single stone column with and without geosynthetic encasement. In *Proceedings of the 2nd international symposium on Asia Urban GeoEngineering*. (Springer, 2018).
33. Ng, K. Numerical study on bearing capacity of single stone column. *Int. J. Geo-Engineering*. **9** (1), 9 (2018).
34. Fattah, M. Y. & Majeed, Q. G. Finite element analysis of geogrid encased stone columns. *Geotech. Geol. Eng.* **30** (4), 713–726 (2012).
35. El-Garhy, B., Galil, A. A. & Mari, M. Analysis of flexible raft resting on soft soil improved by granular piles considering soil shear interaction. *Comput. Geotech.* **94**, 169–183 (2018).
36. Zarazvand, B. & Frankovska, J. Performance evaluation of stone columns in fine soil conditions: A fem-based case study. *Baltic J. Road. Bridge Eng.* **20** (1), 114–142 (2025).
37. Cai, X. et al. Dynamic behavior of GESC groups in sand under sinusoidal loading: A continuum-discrete coupled analysis. *Int. J. Numer. Anal. Methods Geomechan.* (2025).
38. Abdelhamid, M., Ali, N. & Abdelaziz, T. Experimental study on the behavior of floating encased stone columns in collapsible soils. *Indian Geotech. J.* pp. 1–22. (2025).
39. Filz, G. M. et al. Settlement and vertical load transfer in column-supported embankments. *J. Geotech. GeoEnviron. Eng.* **145** (10), 04019083 (2019).
40. Deshpande, T. D. et al. Analysis of railway embankment supported with geosynthetic-encased stone columns in soft clays: a case study. *Int. J. Geosynth. Ground Eng.* **7** (2), 43 (2021).
41. Al-Rkaby, A. H. Performance of Zeolite-Based Soil–Geopolymer mixtures for geostructures under eccentric loading. *Infrastructures* **9** (9), 160 (2024).
42. Castro, J. & Sagaseta, C. Consolidation around stone columns. Influence of column deformation. *Int. J. Numer. Anal. Meth. Geomech.* **33** (7), 851–877 (2009).
43. Rochanavibhata, U. et al. Consolidation behavior of silty sand improved by stone column. *Transp. Infrastr. Geotechnol.* **12** (1), 25 (2025).
44. Brink, R. & Timms, A. Weight, density, absorption, and surface moisture. (1966).
45. Wang, X. et al. Installation behavior of an underwater rammed stone column in clay. *Acta Geotech.* **19** (5), 3213–3228 (2024).
46. Ambily, A. & Gandhi, S. R. Behavior of stone columns based on experimental and FEM analysis. *J. Geotech. GeoEnviron. Eng.* **133** (4), 405–415 (2007).
47. Al-Adhadh, A. R. et al. Improving the shear strength and compressibility of sandy soil by utilizing calcined shale and cement. *Civil Environ. Eng.* **28** (1), 23–37 (2025).
48. Dawood, A. O., Sangoor, A. J. & Al-Rkaby, A. H. Behavior of tall masonry chimneys under wind loadings using CFD technique. *Case Stud. Constr. Mater.* **13**, e00451 (2020).
49. Al-Adhadh, A. R. et al. Supplementary cementitious materials in sandy soil improvement: A review. *J. Building Pathol. Rehabil.* **9** (2), 138 (2024).

Acknowledgements
The author extends the appreciation to the Deanship of Postgraduate Studies and Scientific Research at Majmaah University for funding this research work through the project number ER-2025-2229.

Author contributions
A. Almutairi is the sole author of this study and was responsible for all aspects of the research, including conceptualization, methodology, data collection, analysis, interpretation, manuscript writing, and revision. The author has read and approved the final version of the manuscript.

Funding
This research received grant under Project Number No. ER-2025-2229.

Declarations

Competing interests
The authors declare no competing interests.

Additional information
Correspondence and requests for materials should be addressed to A.A.

Reprints and permissions information is available at www.nature.com/reprints.

Publisher's note Springer Nature remains neutral with regard to jurisdictional claims in published maps and institutional affiliations.